

ELECTRON CLOUD SIMULATIONS IN THE FERMILAB BOOSTER*

S.A.K. Wijethunga [†], A.P. Schreckenberger, C.Y. Tan
 Fermi National Accelerator Laboratory, Batavia, Illinois, USA

Abstract

As part of Fermilab's Proton Improvement Plan-II (PIP-II), the Fermilab Booster synchrotron will operate at a higher intensity, increasing from 4.5×10^{12} to 6.7×10^{12} protons per pulse (ppp). A potential challenge for achieving high intensity performance arises from rapid transverse instabilities induced by electron cloud (EC). This research presents EC simulations using PyECLLOUD, which is an advanced computational tool that incorporates measurements of the secondary electron yield (SEY) from the Booster's combined function magnet material. By systematically varying beam parameters in PyECLLOUD, such as bunch structure, SEY, bunch length, and intensity, it becomes possible to forecast the impact of EC effects on the beam stability of the PIP-II era Booster.

INTRODUCTION

In particle accelerators, free electrons are always present within vacuum chambers for various reasons, including ionization of residual gas molecules and stray beam particles colliding with chamber walls. Electromagnetic fields from the beam can accelerate these electrons to energies ranging from several hundreds of electron volts to a few thousand electron volts, depending on beam intensity. When these electrons collide with chamber walls, secondary electrons are produced based on their impact energy and the Secondary Electron Yield (SEY) of the surface. This cycle, particularly with closely spaced bunches of proton beams, can trigger an avalanche effect, generating electron clouds (ECs) [1-2]. These ECs pose significant challenges for high intensity proton accelerators, leading to issues such as transverse instabilities, emittance growth, particle losses, vacuum deterioration, and surface heating within the chamber [3-5].

Earlier research conducted at the Fermilab Recycler facility has shown that combined function magnets possess the capability of confining ECs by the magnetic mirror effect. Simulation findings suggest that ECs gathered over multiple revolutions within these combined function magnets can reach intensities several orders of magnitude greater than those observed within a pure dipole [6,7].

To fulfill the requirements outlined in Fermilab's Proton Improvement Plan-II (PIP-II), the Fermilab Booster [8], a rapid cycling synchrotron (presently @15 Hz, PIP-II@20 Hz) that contains 96 combined function magnets, must supply a high intensity beam of 6.7×10^{12} ppp, marking a 44% increase in current intensity [9]. Consequently, it becomes crucial to detect any indication of the existence of

an EC within the PIP-II era Booster and assess its potential impact on achieving the desired performance.

This paper describes the methodology and findings of SEY measurements performed on Booster combined-function magnet materials and a sequence of simulation studies using the PyECLLOUD program to analyze EC accumulation within the magnet. These simulations varied parameters such as bunch length, SEY, and beam intensity to explore their effects on EC buildup.

SEY MEASUREMENTS

The SEY quantifies the average number of secondary electrons emitted when a single electron strikes a surface. It typically depends on the incident electron energy and incident angle. In particle accelerators, the SEY is a crucial characteristic of the vacuum chamber materials, which exerts a significant influence on the accumulation of free electrons, which ultimately may result in an EC [10,11].

Booster combined function magnets are constructed by stacking steel sheets (SS) with epoxy (Ep) layers in between [8], as shown in Figure 1, to minimize eddy currents. As a result, the accelerated free electrons within the vacuum chamber can potentially interact with both the SS and Ep components of these magnets. Hence, the SEY strength (δ_{SEY}) of the combined function magnet material should be considered as the combination of both δ_{SEY} of SS and δ_{SEY} of Ep. Note: the sample utilized in this study has not been exposed to the beamline and, thus, has not undergone any conditioning.

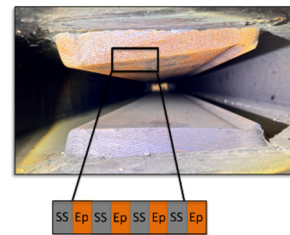


Figure 1: Picture of Booster combined function magnet elaborating the SS and Ep layers.

SEY Test Stand

The SEY test stand is a dedicated setup situated in the XGW-003 area of the Fermilab Accelerator Division building designed to measure the δ_{SEY} of various samples. As shown in Figure 2, it consists of a Kimball electron gun driven by a 1022B-type power supply, a vacuum chamber with pumping equipment (to keep the pressure $< 1 \times 10^{-5}$ torr), and a Keithley pico-ammeter. The system configuration is primarily controlled through the electron gun power supply. The 1st anode voltage is held at 95.3 V. The electron energy ramps from 0 to 1.5 kV in increments of 25 eV, and the focus voltage follows this ramp with empirically

* This manuscript has been authored by Fermi Research Alliance, LLC under Contract No. DE-AC02-07CH11359 with the U.S. Department of Energy, Office of Science, Office of High Energy Physics.

[†] swijethu@fnal.gov

determined set points that mostly follow a shifted tanh function. The leakage current magnitude of the test stand system generally ranges between 3 and 12 pA, depending on the bias voltage applied, and the grid voltage is set such that measured currents are at least an order of magnitude larger. This typically leads to an applied grid voltage between 12.0 and 14.3 V. A 3x3 grid sweep over the sample surface is introduced through the application of deflection voltages that also scale with energy. The full scan procedure takes roughly an hour per measurement to complete.

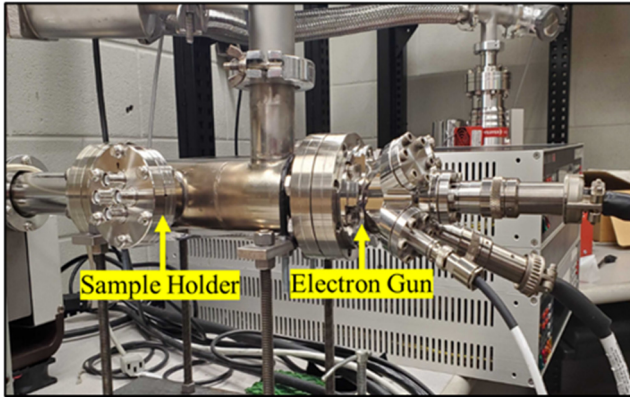


Figure 2: SEY test stand.

A special sample holder was designed for this measurement, as shown in Figure 3(b), to collect the maximum current from the Ep side of the sample.

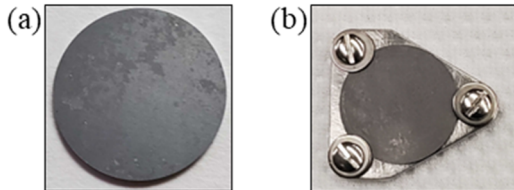


Figure 3: (a) SS sample. (b) Ep side of the sample mounted into the holder.

According to our technique, the δ_{SEY} of a sample is obtained by using the following equation,

$$\delta_{SEY} = \frac{I_{SEY}}{I_p} = \frac{I_+ - I_-}{I_+} \quad (1)$$

In order to collect the primary electrons ($I_p = I_+$), the sample was biased at +150 V. This forced the recapture of the secondary electrons escaping from the surface. This current is ideally equivalent to the current from the gun. Afterward, the bias was changed to -20 V to repel the low-energy secondary electrons to obtain I_- .

SEY Measurement Results

Figure 4 shows the SEY measurement for the SS side of the sample on three different days with slightly different

vacuum levels compared with a standard 316 Stainless steel sample.

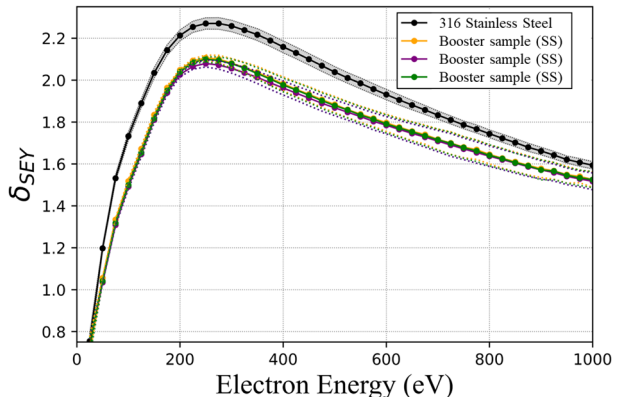


Figure 4: δ_{SEY} of the SS side of the Booster magnet compared with the δ_{SEY} of the 316 Stainless steel sample.

Figure 5 shows the SEY measurements of both SS and Ep sides.

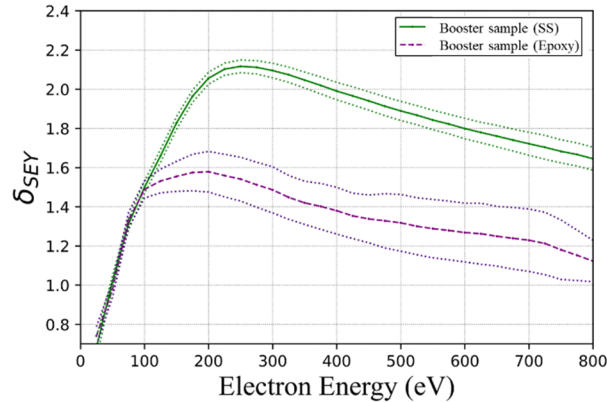


Figure 5: δ_{SEY} of the SS and Ep sides.

The measurements shown in Figure 4 help us validate our measurement technique by comparing them against the standard 316 Stainless steel measurement. Figure 5 shows that the δ_{SEY} of SS lies around 2.1 and δ_{SEY} of Ep lies around 1.6. However, due to beam pipe conditioning over the years, we assume that the δ_{SEY} of the magnet material has decreased from our measurements.

SIMULATIONS

To model the EC accumulation within a combined function magnet in the Booster synchrotron, PyECLOUD program was utilized [12]. Table 1 details the primary input parameters employed in the simulations. The cross section of the combined function magnet was modeled as a rectangle featuring dipole and quadrupole magnetic fields. Initially, the number of electrons was set at 10^4 .

Table 1: Common Input Parameters in Simulations

Parameter	Transition	Injection
Beam energy [GeV]	4.2	0.4
Bunch spacing [ns]	19.2	26.4

Simulations were carried out by varying the δ_{SEY} of the magnet material, bunch length, and intensity of the beam. Figure 6 shows the EC build-up for a range of δ_{SEY} of the magnet material at injection (bunch length, $\sigma = 0.57$ [m]) and at transition (bunch length, $\sigma = 0.25$ [m]) for PIP-II intensity 6.7×10^{12} . PyECLLOUD shows that the EC accumulated only when $\delta_{SEY} > 1.9$ at injection, and the accumulation rate increased as δ_{SEY} increases.

Based on the correlation presented in Ref. [13] regarding the tune shift (ΔQ) and the associated electron cloud density (ρ), for a δ_{SEY} of 2.1, the maximum tune shift calculated is approximately 0.007 at injection and 0.003 at transition.

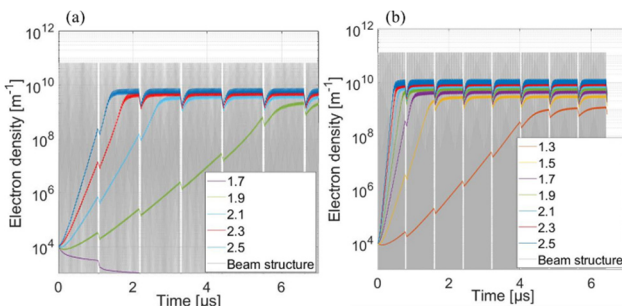


Figure 6: EC build-up for different δ_{SEY} of the magnet material. (a) at injection and (b) at transition.

Figure 7 shows the EC build-up for different bunch lengths at injection and at transition for $\delta_{SEY} = 2.1$ and intensity 6.7×10^{12} . The saturation of the EC density remains nearly unchanged regardless of the bunch length at both injection and transition. The corresponding theoretical maximum tune shift is approximately 0.02 at injection and around 0.005 at transition, only when the bunch length is 0.1 m (rms).

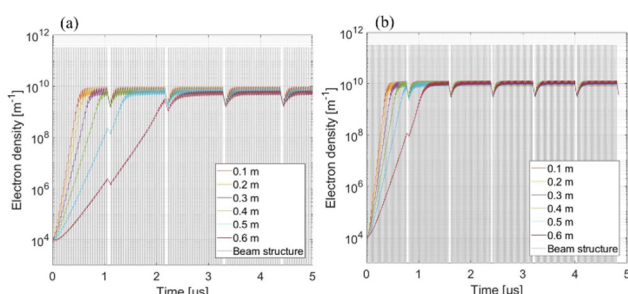


Figure 7: EC build-up for different bunch lengths. (a) at injection and (b) at transition.

Figure 8 shows the EC build-up for different beam intensities for single notch and opposite notch described in Ref. [14] for $\delta_{SEY} = 1.8$. PyECLLOUD simulations did not show

EC accumulation near injection with a $\delta_{SEY} = 1.8$ and a bunch length of 0.57 m (rms). Furthermore, EC saturation remains consistent across all high intensity beams, regardless of their specific bunch structure, indicating that notch configurations were minimally effective in mitigating EC presence. According to theory, the maximum tune shift near the transition is estimated to be around 0.001 for 6.7×10^{12} beam intensity.

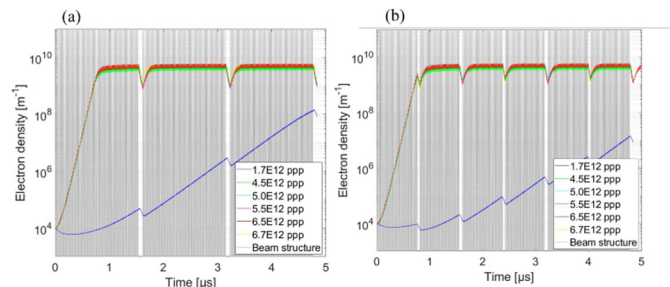


Figure 8: EC build-up for different beam intensities (a) single notch and (b) opposite notch.

CONCLUSION

In conclusion, this study successfully conducted SEY measurements on both the SS and Ep sides of the combined function magnet material, $\delta_{SEY}(\text{Ep}) \approx 1.6$ and $\delta_{SEY}(\text{SS}) \approx 2.1$. However, due to the vacuum chamber conditioning over time, we assume that the δ_{SEY} of the magnet material has reduced from our initial measurements. Based on the previous experience, analysis of tune shifts indicates that they are not significant enough to be a primary cause for instabilities. Furthermore, observations suggest that the density of accumulated electron clouds remains nearly constant for intensities exceeding 4.5×10^{12} ppp. Despite operating the Booster at 6.1×10^{12} ppp and experiencing instabilities attributed to impedances controlled by dampers and chromaticities, the contribution to instability from EC effects appears minimal. Therefore, it can be inferred that EC accumulation is not anticipated to pose a significant problem in the PIP-II era Booster.

ACKNOWLEDGMENT

We are grateful to Salah Chaurize (BD/PS) and Kevin Duel (ACTD/MSD) for their help.

REFERENCES

- [1] H. Fukuma, K. Cornelis, F.-J Decker, R. Macek, E. Metral, and W. Fischer, in *Proceedings of ECLOUD '02, CERN, Geneva, 2002*.
- [2] G. Rumolo *et al.*, “Electron cloud effects on beam evolution in a circular accelerator,” *Physical Review Special Topics - Accelerators and Beams*, vol. 6, no. 8, Aug. 2003. doi:10.1103/physrevstab.6.081002
- [3] G. Arduini, K. Cornelis, W. Hoefle, G. Rumolo, and F. Zimmermann, “The Electron Cloud Instability of the LHC Beam in the CERN SPS”, in *Proc. PAC'03*, Portland, OR, USA, May 2003, paper RPPB011, pp. 3038-3040.
- [4] G. Iadarola *et al.*, “Analysis of the Electron Cloud Observations with 25 ns Bunch Spacing at the LHC”, in *Proc.*

IPAC'14, Dresden, Germany, Jun. 2014, pp. 1410-1412.
 doi:10.18429/JACoW-IPAC2014-TUPME027

- [5] W. Fischer *et al.*, “Electron cloud observations and cures in the Relativistic Heavy Ion Collider,” *Physical Review Special Topics - Accelerators and Beams*, vol. 11, no. 4, Apr. 2008. doi:10.1103/physrevstab.11.041002
- [6] S. A. Antipov, P. Adamson, A. Burov, S. Nagaitsev, and M.-J. Yang, “Fast instability caused by electron cloud in combined function magnets,” *Phys. Rev. Accel. Beams*, vol. 20, no. 4, Apr. 2017.
 doi:10.1103/physrevaccelbeams.20.044401
- [7] J. S. Eldred *et al.*, “Fast Transverse Instability and Electron Cloud Measurements in Fermilab Recycler”, in *Proc. HB'14*, East Lansing, MI, USA, Nov. 2014, paper THO4LR04, pp. 419-427.
- [8] Booster rookie book,
https://operations.fnal.gov/rookie_books/Booster_V4.1.pdf
- [9] S. Holmes *et al.*, “Long Term Plans to Increase Fermilab's Proton Intensity to Meet the Needs of the Long Baseline Neutrino Program”, in *Proc. IPAC'16*, Busan, Korea, May 2016, pp. 1010-1013.
 doi:10.18429/JACoW-IPAC2016-TU0AA03
- [10] S. Liu, Y. Liu, W. Liu, G. Pei, P. Wang, L. Zeng, X. Sun “Experimental studies on secondary electron emission characteristics of accelerator chamber materials,” in *Proceedings of ECLOUD'18*, La Biodola, Italy, 2018.
- [11] Y. Ji, L. K. Spentzouris, and R. M. Zwaska, “Secondary Electron Yield Measurement and Electron Cloud Simulation at Fermilab”, in *Proc. IPAC'15*, Richmond, VA, USA, May 2015, pp. 629-632.
 doi:10.18429/JACoW-IPAC2015-MOPMA039
- [12] G. Iadarola, PyECLOUD Version 8.6.0, CERN, 2021.
- [13] S. Wijethunga *et al.*, “Electron cloud measurements in Fermilab booster”, in *Proc. IPAC'23*, Venice, Italy, May 2023, pp. 2858-2861.
 doi:10.18429/JACoW-IPAC2023-WEPA093
- [14] S. A. K. Wijethunga, J. S. Eldred, E. Pozdeyev, and C.-Y. Tan, “Electron Cloud Measurements in Fermilab Booster”, in *Proc. NAPAC'22*, Albuquerque, NM, USA, Aug. 2022, pp. 556-559. doi:10.18429/JACoW-NAPAC2022-WEXD6